Title
Induction of early neural precursors and derivation of tripotent neural stem cells from human pluripotent stem cells under xeno-free conditions

Journal
The Journal of Comparative Neurology, 522(12)

ISSN
1550-7149

Authors
Nguyen, Hal X
Nekanti, Usha
Haus, Daniel L
et al.

Publication Date
2014-08-15

DOI
10.1002/cne.23604

Peer reviewed

Induction of Early Neural Precursors and Derivation of Tripotent Neural Stem Cells From Human Pluripotent Stem Cells Under Xeno-Free Conditions

Hal X. Nguyen,[1,2,3,4]* Usha Nekanti,[4] Daniel L. Haus,[2,3] Gabrielle Funes,[4] Denisse Moreno,[4] Noriko Kamei,[4] Brian J. Cummings,[1,2,3,4] and Aileen J. Anderson[1,2,3,4]*

[1]Physical Medicine & Rehabilitation, University of California, Irvine, California
[2]Anatomy and Neurobiology, University of California, Irvine, California
[3]Sue and Bill Gross Stem Cell Research Center, University of California, Irvine, California
[4]Institute for Memory Impairments and Neurological Disorders, University of California, Irvine, California

ABSTRACT

Human embryonic stem cells (hESC) and induced pluripotent stem cells (hiPSC) can differentiate into many cell types and are important for regenerative medicine; however, further work is needed to reliably differentiate hESC and hiPSC into neural-restricted multipotent derivatives or specialized cell types under conditions that are free from animal products. Toward this goal, we tested the transition of hESC and hiPSC lines onto xeno-free (XF) / feeder-free conditions and evaluated XF substrate preference, pluripotency, and karyotype. Critically, XF transitioned H9 hESC, Shef4 hESC, and iPS6-9 retained pluripotency (Oct-4 and NANOG), proliferation (MKI67 and PCNA), and normal karyotype. Subsequently, XF transitioned hESC and hiPSC were induced with epidermal growth factor (EGF) and basic fibroblast growth factor (bFGF) to generate neuralized spheres containing primitive neural precursors, which could differentiate into astrocytes and neurons, but not oligoprogenitors. Further neuralization of spheres via LIF supplementation and attachment selection on CELLstart substrate generated adherent human neural stem cells (hNSC) with normal karyotype and high proliferation potential under XF conditions. Interestingly, adherent hNSC derived from H9, Shef4, and iPS6-9 differentiated into significant numbers of O4+ oligoprogenitors (~20–30%) with robust proliferation; however, very few GalC+ cells were observed (~2–4%), indicative of early oligodendrocytic lineage commitment. Overall, these data demonstrate the transition of multiple hESC and hiPSC lines onto XF substrate and media conditions, and a reproducible neuralization method that generated neural derivatives with multipotent cell fate potential and normal karyotype. J. Comp. Neurol. 000:000–000, 2014.

INDEXING TERMS: hESC; hiPSC; human neural stem cells; neuralization; oligoprogenitors; xeno-free

Efficient derivation and expansion of multipotent neural derivatives under conditions free from animal products (xeno-free, XF) is a major challenge for potential cell therapies using pluripotent origin stem cells (e.g., human embryonic stem cells [hESC] and induced pluripotent stem cells [hiPSC]). Neuralization protocols capable of generating neural derivatives with some potential to differentiate into astrocytes and neurons (Zhang et al., 2001; Denham and Dottori, 2009), or specific neural progenitors that give rise to motor neurons (Li et al., 2005; Erceg et al., 2008; Chambers et al., 2009; Ebert et al., 2009), dopaminergic neurons (Zhang and Zhang, 2010; Schwartz et al., 2012; Swistowski and Zeng, 2012), or oligodendrocytes (Okamura et al., 2007; Hatch et al., 2009; Erceg et al., 2013), have been reported. However, neural derivatives generated from protocols such as embryoid body (EB) and neural rosette formation can be unstable and difficult to expand efficiently (Guillaume and Zhang, 2008; Ebert

Grant sponsor: California Institute for Regenerative Medicine (CIRM); Grant numbers: RB2-01496; TR2-01767; TG2-01152.

*CORRESPONDENCE TO: Hal X. Nguyen, PhD, University of California Irvine, 2101 Gross Hall Stem Cell Research Center, Irvine, CA 92697. E-mail: hnguyen@uci.edu or Aileen Anderson, PhD, University of California Irvine, 2030 Gross Hall Stem Cell Research Center, Irvine, CA 92697. E-mail: aja@uci.edu

Received September 4, 2013; Revised April 4, 2014;
Accepted April 4, 2014.
DOI 10.1002/cne.23604
Published online April 9, 2014 in Wiley Online Library (wileyonlinelibrary.com)

et al., 2009). Moreover, the resulting neural precursors are typically exposed to undefined factors in culture. In fact, recent advances for cell differentiation into human neural stem cells (hNSC) and specific neural progenitors or cell types have been made predominantly from cells maintained under conditions containing undefined animal-derived products, which can increase the risk of host immune responses, graft rejection, or infection by nonhuman pathogens (Cobo et al., 2005; Martin et al., 2005; Skottman and Hovatta, 2006). Furthermore, animal-derived products may have added unknown effects on cell characteristics (e.g., proliferation, differentiation, etc.) in vitro and in vivo. Hence, establishing XF cell culture conditions and protocols to neuralize hESC/hiPSC is an important step to further the development of therapeutically relevant cell lines.

To enhance the efficiency and control of neural derivative generation under XF conditions, defined factors have been used to directly induce hESC neuralization into lineage committed cells such as motor neurons, dopaminergic neurons, or oligoprogenitors, including retinoic acid, sonic hedgehog, and the BMP and/or SMAD signaling inhibitor noggin (Li et al., 2005; Chiba et al., 2008; Wada et al., 2009; Sundberg et al., 2011). However, the practicality of these potent morphogens may be limited by their possible association with chromosomal instability/aneuploidy, as has been reported for retinoic acid-treated hESC/hiPSC (Sartore et al., 2011). In parallel, advances have established defined and XF systems for pluripotent hESC/hiPSC culture including mTeSR1, StemPro, TeSR2, NutriStem, RegES, and KO-SR XF/GF cocktail, which can be used with XF human recombinant laminin substrate (LN-511), human fibroblast feeder substrate, or XF and feeder-free substrates such as StemAdhere or CELLstart matrix (Rajala et al., 2010; Nagaoka et al., 2010; Bergstrom et al., 2011; Swistowski and Zeng, 2012). However, relatively little is known about long-term propagation and, critically, neural derivation of hESC/hiPSC under XF/feeder-free conditions. In the few studies that have reported the feasibility of maintaining hESC/hiPSC and neural derivatives under "XF" or "XF defined" conditions, pluripotent cells were maintained in the presence of bovine serum albumin (BSA), and neural derivatives were expanded in media containing B27, both of which contain animal products, and the karyotype of these neural derivatives was not reported (Okuno et al., 2009; Swistowski et al., 2009; Rajala et al., 2010).

In this study, we tested the transition of three hESC lines and one hiPSC line onto XF/feeder-free conditions, evaluating XF substrate preference, pluripotency marker expression, and karyotype stability. We then subjected XF transitioned hESC and hiPSC lines to an XF-adapted neuralization protocol, followed by maintenance of the resulting neural derivatives as either spheres (termed neuralized spheres) or under adherent conditions (termed adherent hNSC). Finally, we compared the resultant neuralized spheres and adherent hNSC for neural differentiation based on immunocytochemistry, expression of neural lineage markers in quantitative polymerase chain reaction (PCR), and flow cytometry. One-step XF/feeder-free transition of hESC/hiPSC onto CELLstart or StemAdhere substrate yielded stable colonies that retained pluripotency, proliferation, and normal karyotype for at least seven passages. Direct differentiation of these hESC and hiPSC using epidermal growth factor (EGF) and basic fibroblast growth factor (bFGF) generated neuralized spheres containing primitive neural precursors that differentiated into astrocytes and neurons, but not oligoprogenitors. Further differentiation of neuralized spheres via LIF supplementation and attachment selection on CELLstart substrate generated adherent hNSC with normal karyotype and high proliferation potential under XF conditions. Critically, adherent hNSC from all cell lines acquired robust potential for oligodendrocytic lineage differentiation.

MATERIALS AND METHODS

hESC/hiPSC lines and conditions

H1 (WA01) and H9 (WA09) hESC, and integration-free hiPSC (DF6-9-9T.B; iPS6-9) lines were obtained from WiCell Research Institute (Madison, WI). The Shef4 hESC line was kindly supplied by Dr. Harry Moore (Sheffield, UK). Prior to the XF transition described below, H9 and Shef4 were maintained on mouse embryonic fibroblasts (MEF) (Millipore, Bedford, MA) feeder cells with non-XF hESC media (DMEM-F12, 20% KOSR, 1 mM L-glutamine, 0.1 mM B-ME, 1% NEAA, 4 ng/ml bFGF); H1 and iPS6-9 lines were maintained on Matrigel (BD Biosciences, San Jose, CA)-coated surfaces (diluted 1:30 with KnockOut DMEM) in defined mTeSR1 media (StemCell Technologies, Vancouver, BC, Canada). MEF were seeded on a 0.1% gelatin-coated surface of T25 or 6-well plates in MEF media (DMEM, 10% FBS, 2 mM L-glutamine, and 1% NEAA) 1 day before plating H9 and Shef4 hESC. Matrigel was plated on the surface of 6-well plates before plating HI and iPS6-9. All cells were cultured at 37°C in a 95% air / 5% CO_2 humidified incubator, and were mechanically passaged after confluency.

Xeno-free transition and conditions for hESC/hiPSC

One-step transition of hESC/hiPSC onto XF conditions was accomplished via simultaneous replacement

of media and substrate with XF media and XF substrate. Based on availability and manufacturers' recommendations to optimize XF conditions, two XF systems were tested for all lines. Briefly, non-tissue culture treated 6-well plates (Corning, Corning, NY) were incubated with StemAdhere XF (Primorigen; diluted to 12.5 μg/ml in phosphate-buffered saline [PBS] with Ca2+ and Mg2+) or CELLstart (Invitrogen, La Jolla, CA; 1:100 diluted in PBS with Ca2+ and Mg2+) for 1 hour at 37°C. In this one-step transition protocol, H9/Shef4 hESC on MEF and H1 hESC/iPS6-9 on Matrigel were passaged onto StemAdhere XF-coated plates in TeSR2 media (StemCell Technologies) or CELLstart-coated plates in XF hESC media (Invitrogen).

Immediately after XF transition, confluent cell colonies (Passage 0) on both XF systems were fixed and assessed for retained pluripotency via cell morphology and expression of Oct-4 and SSEA4. Briefly, colonies of hESC or hiPSC were washed with PBS before being incubated for 30 minutes in blocking solution containing 10% goat serum and 0.1% Triton-X. Primary antibody solution containing rabbit anti-Oct-4 (Abcam, Cambridge, MA; 1:200) and mouse anti-SSEA4 (Abcam; 1:100) was incubated with cells for 1 hour at room temperature. Cells were washed twice in PBS and incubated in secondary antibody solution containing anti-mouse Alexa 488 (Invitrogen; 1:500) and antirabbit Alexa 555 (Invitrogen; 1:500). All cells were identified using a nucleic-fluorescent dye Hoechst 33342 (1:1,000, Invitrogen). Once pluripotency was determined after initial XF transition, long-term passaging of hESC/hiPSC was carried out for at least seven passages under the XF condition before cells were tested for retained pluripotency as described above and chromosomal stability via karyotype assessment (Cell Line Genetics, Madison, WI).

Derivation and maintenance of neuralized spheres and adherent hNSC under xeno-free conditions

Generation of neuralized spheres from XF-transitioned hESC and hiPSC was carried out essentially as described previously (Ebert et al., 2009). Briefly, cell colonies were expanded to at least 70% confluency on XF CELLstart or XF StemAdhere substrate in a 6-well culture plate. Spontaneously differentiated colonies or cells were manually removed with a sterile 18G needle under a microscope via gentle scraping. XF hESC media or TeSR2 media was aspirated and the remaining undifferentiated cell colonies were washed once with PBS. One ml of fresh defined neural induction media (X-Vivo based media [Lonza, Basel, Switzerland], 0.1 μg/ml human bFGF, 0.1 μg/ml human EGF, 5 μg/ml heparin, 2% B27 supplement) or XF neural induction media (X-Vivo based media, 0.1 μg/ml human bFGF, 0.1 μg/ml human EGF, 1% N2 supplement) was added to each well and colonies were scraped from the substrate surface with the tip of a 5-ml serological pipette. Cell aggregates were placed directly into Ultra-Low Attachment Surface flasks (Corning) and cultured as cell suspensions in defined neural induction media or XF neural induction media for 7 days to form neuralized spheres at Passage E0. Passage of neuralized spheres was designated as E, which a previous study referred to as "EZsphere" (Ebert et al., 2013). Neuralized spheres (E0) were maintained in suspension for up to 3 more days until appropriate size (~1 mm) before passaging 1-to-2 via mechanical dissociation. Briefly, spheres were collected and resuspended in 500 μl PBS. Spheres were gently triturated using a P200 pipette until they were dissociated evenly. Pelleted cells were resuspended in an appropriate volume of defined or XF neural induction media and were cultured in suspension as Passage E1. Most neuralized spheres at E1 to E4 were cryopreserved in cold XF cryo-medium (4% human serum albumin and 7.5% DMSO) that contained human serum albumin (HSA) in place of bovine serum albumin (BSA). The rest of the spheres at E3 to E6 were 1) lysed for RNA collection, 2) differentiated in neural differentiation media on PLL/Laminin, or 3) placed in XF hNSC media (see below) to proceed with the generation of adherent hNSC.

Generation of adherent hNSC began with the placement of neuralized spheres (E3 to E6) in XF hNSC media (X-Vivo based media, 0.1 μg/ml human bFGF, 0.1 μg/ml human EGF, 0.01 μg/ml human LIF, 1% N2 supplement) and cultured in suspension for 5 days. Using one 6-well plate precoated with CELLstart (1:100 in $MgCl_2$ PBS), cells were attached by plating 5–10 spheres/well for an additional 5–7 days until the migrating cells from attached spheres were expanded to confluency in XF hNSC media to generate monolayer adherent hNSC (Passage M1). Passage of adherent hNSC was designated as M, which stood for "monolayer" adherent hNSC. Most M1 adherent hNSC were cryopreserved as M1 stocks in cold XF cryo-medium (4% HSA and 7.5% DMSO). The remaining M1 wells were passaged (1:6) onto CELLstart-coated wells. All adherent hNSC were passaged via a brief 1-minute incubation (1 ml/well) with XF Trple Trypsin (Invitrogen). Trple was then inactivated with 2 ml of XF hNSC media per well and cells were detached from the surface by gentle pipetting. Collected M2 adherent hNSC were suspended in XF hNSC media and plated onto CELLstart-coated wells (2 ml/well) for 5–7 days until

TABLE 1.
List of Antibodies Used for Immunocytochemistry and Flow Cytometry

Antibody	Immunogen	Manufacturer (Cat. # and Research Resource ID)
Immunocytochemistry		
anti-Oct-4	Synthetic peptide of human Oct-4	Abcam (ab19857, RRID:AB_445175, rabbit polyclonal)
anti-SSEA4	Human embryonal carcinoma 2102Ep	Abcam (ab16287, RRID:AB_778073, mouse monoclonal)
anti-β-tubulin III	Microtubules from rat brain	Covance (MMS435P, RRID:AB_10063408, mouse monoclonal)
anti-GFAP	GFAP from human brain	Dako (M0761, RRID:AB_2109952, mouse monoclonal)
anti-O4	Bovine corpus callosum homogenate	Millipore (MAB345, RRID:AB_94872, mouse monoclonal)
anti-Galactocerebroside (GalC)	Bovine synaptic plasma membranes	Millipore (MAB342, RRID:AB_94857, mouse monoclonal)
anti-nestin	Human fusion protein	Millipore (MAB5326, RRID:AB_2251134, mouse monoclonal)
anti-NeuN	GST-tagged recombinant protein	Millipore (ABN78, RRID:AB_10807945, rabbit polyclonal)
Flow Cytometry		
anti-O4 PE	Oligodendrocyte marker O4	R&D Systems (FAB1326P, RRID:AB_664169, mouse monoclonal)
anti-GalC A488	Bovine synaptic plasma membranes	Millipore (MAB342A4, RRID:AB_94857, mouse monoclonal)

confluent. Some M2 adherent hNSC were 1) lysed for RNA collection, 2) passaged to a CELLstart-coated T25 flask for karyotype analysis (Cell Genetics) at M3, or 3) passaged in the neural differentiating conditions described below.

Neural differentiation of neuralized spheres and adherent hNSC

Neuralized sphere-dissociated cells (E3 to E6) and adherent hNSC (M3 to M4) were differentiated in neural differentiation media on PLL/laminin substrate for up to 14 days in vitro (14DIV). Consistent with the dissociation of adherent hNSC to yield single cell suspensions for neural differentiation, suspended spheres were also dissociated with Trple followed by mechanical trituration. Neuralized sphere-dissociated cells and adherent hNSC were passaged and plated onto wells of 6-well plates and 8-well chamber slides that were precoated first with PLL (1:10 with dH2O) overnight followed by 2 hours laminin (1:100 with PBS) before cell seeding. Cells were plated at 2,000 cells per well for 8-well chamber slides (150 μl/well) and 25,000 cells per well for 6-well plates (1.5 ml/well) in XF hNSC media. On the following day, XF hNSC media was removed, cells were washed once with X-Vivo Media, and neural differentiation media (X-Vivo based media, 10 ng/ml human BDNF, 10 ng/ml human GDNF, 1 ng/ml human bFGF, 10 μg/ml Cipro, 2 μg/ml heparin, 63 μg/ml NAC, 1% N2 supplement, 2% B27 supplement) was added to the cells. Every 4 days a small additional volume of differentiation media was added to each slide well (50 μl/well) or plate well (350 μl/well) through 14DIV. At 14DIV, cells in chamber slides were fixed with 2% paraformaldehyde for immunocytochemistry analysis. Cells in plates were detached with Trple, lysed for RNA sample collection, or fixed (2% paraformaldehyde) for EDU-incorporated cell proliferation and flow cytometry analyses. For each cell line, neural differentiation experiments of neuralized spheres and adherent hNSC reflect data averaged across three biological replicates; each biological replicate was performed using technical triplicates by separate individuals.

Antibody characterization

Antibodies used for fluorescent immunolabeling and flow cytometry of hESC/hiPSC derived neuralized spheres and adherent hNSC are listed in Table 1. Anti-Oct-4 and anti-SSEA4 were characterized previously to specify human stem cell pluripotency (Kohen et al., 2009; Xue et al., 2013). Anti-nestin was shown to specifically react with human Nestin (Findikli et al., 2005) and was not reactive to rodent nestin. Cells of neuronal lineage were identified via anti-β-tubulin III and anti-NeuN. Anti-β-tubulin III was characterized to be highly reactive to neuron specific Class III β-tubulin (βIII) (Jouhilahti et al., 2008). Anti-NeuN recognized the DNA-binding, neuron-specific protein NeuN in CNS and PNS neuronal cell types (Chera et al., 2002). Anti-glial fibrillary acid protein (GFAP) was characterized and was shown to label GFAP in astrocytes and cells of astrocytic origin (Leroy et al., 2001). Anti-O4 and Anti-GalC were shown to bind specifically with oligoprogenitors (McClain et al., 2012) and oligodendrocytes (Swistowski and Zeng, 2012), respectively. Furthermore, the specificity of these antibodies was validated for flow cytometric analyses using IgG or IgM isotypes as described below.

Immunolabeling of neuralized spheres and adherent hNSC after neural differentiation

After 14DIV in neural differentiation media, sphere-dissociated cells and adherent hNSC were fixed and

immunolabeled for markers associated with astroctyes, neurons, and oligodendrocytes. Briefly, fixed cells slides were washed with PBS and incubated for 30 minutes in blocking buffer (3% BSA, 2% gelatin and 0.1% Triton-X) (Nguyen and Tidball, 2003). Following several washes with PBS, cells were incubated in mouse anti-β-tubulin III (Covance, Denver, PA; 1:250), rabbit anti-GFAP (Dako, Carpinteria, CA; 1:500), mouse anti-O4 (Millipore; 1:100), mouse anti-GalC (Millipore; 1:100); Mouse anti-nestin (Millipore; 1:200), rabbit anti-NeuN (Millipore; 1:500) solution for 1 hour (Table 1). Immunoreactive cells were identified using a goat antimouse IgG Alexa 488 (Invitrogen; 1:500) or goat antirabbit IgG Alexa 555 (Invitrogen; 1:500). All cells were also identified using a nucleic-fluorescent dye, Hoechst 33342 (1:1,000, Invitrogen). All slides were mounted with glass coverslips using Flouromount-G and fluorescent images were taken from a representative set of three biological replicates which included technical triplicates.

Real-time PCR

Pluripotent and neural gene expression profiles were characterized using quantitative PCR (qPCR) custom arrays (ABI Life Technologies, Foster City, CA). Total RNA was isolated from cell culture samples using a RNeasy Mini Kit (Qiagen, Chatsworth, CA). To eliminate traces of genomic DNA, the RNA samples were treated with DNA-free DNase I (Ambion, Austin, TX). Each cDNA was generated using a High Capacity cDNA Reverse Transcription Kit according to the manufacturer's instructions (ABI Life Technologies), and subsequent qPCR reactions were completed on an Applied Biosystems (Foster City, CA) ViiA 7 Real-Time PCR System. Relative expression levels were calculated using the comparative C_t method, based on the expression level of each target gene and housekeeping gene. Housekeeping gene 18S rRNA was used to normalize all target genes and show quantification values as cycle threshold or as heat maps. Real-time PCR was performed using technical triplicates and reported as a heatmap without statistical analysis.

EDU cell proliferation and flow cytometric assessments

H9, Shef4, and iPS6-9 adherent hNSC were cultured in differentiating conditions for 14DIV as above. 5 μM of EdU (Invitrogen; #C10419) was added at 13DIV to culture media 1 day before cell harvest. Cells were lifted with 1 ml of TrypLE, and 2 ml PBS was added to dilute and inactivate the trypsin. An equal volume of 4% (w/v) paraformaldehyde was then added to fix the cells. Each cell sample (450 μL) was centrifuged at 2,000 RPM for 90 seconds. Pelleted cells were incubated in 500 μL of 1× saponin-based permeabilization wash buffer for 30 minutes at room temperature. Following centrifugation and supernatant removal, a reaction cocktail (consisting of PBS, $CuSO_4$, AF647 Azide, and 1× EdU Buffer Additive according to an EDU Kit, Invitrogen) was added to the cell pellet and cells were dissociated and incubated in the dark for 30 minutes. After a wash, cells were incubated with anti-GalC A488 (Millipore; 500 ng/μL) or anti-O4 PE (R&D Systems, Minneapolis, MN; 100 ng/μL) listed in Table 1, or appropriate IgG or IgM isotype controls for 30 minutes and were washed a final time in 1× saponin permeabilization buffer before cells were analyzed on a BD LSR II Flow Cytometer. Cell viability detected by propidium iodide (Invitrogen) was typically more than 90%; all flow cytometric gates were set using control IgG or IgM isotype labeled cells. The mean values of cells positive for EDU, O4, and GalC as determined by flow cytometry were expressed as percent (± standard error [SE]) relative to control IgG or IgM isotype labeled cells. Each experiment reflects data averaged across three biological replicates; each biological replicate was performed using technical triplicates by separate individuals.

Statistical analysis

One-way analysis of variance (ANOVA) with post-hoc Tukey's multiple comparison tests were used to assess flow cytometric data of % O4+, GalC+, and EDU+ cells for differences between adherent hNSC lines. Prism (v. 5.0a) was used for statistical analysis; significance was defined as $P < 0.05$.

RESULTS

Xeno-free/feeder-free transitioned hESC and hiPSC retain pluripotency and normal karyotype

We first sought to establish XF conditions (i.e., media and substrate) under which hESC and hiPSC could be stably propagated and maintained. Accordingly, the transition of hESC (H1, H9, Shef4) and hiPSC (iPS6-9) into XF conditions was initially implemented using an incremental approach in which hESC/hiPSC were gradually transitioned onto XF substrate followed by XF media replacement; however, this approach was found to be inefficient, with a high rate of spontaneous differentiation. Surprisingly, an alternative one-step transition approach, in which cell substrate and media were simultaneously switched to XF hESC media (Invitrogen) and maintained on XF and feeder-free CELLstart matrix (Invitrogen) or StemAdhere XF (Primorigen) substrate, was highly successful. Interestingly, using this

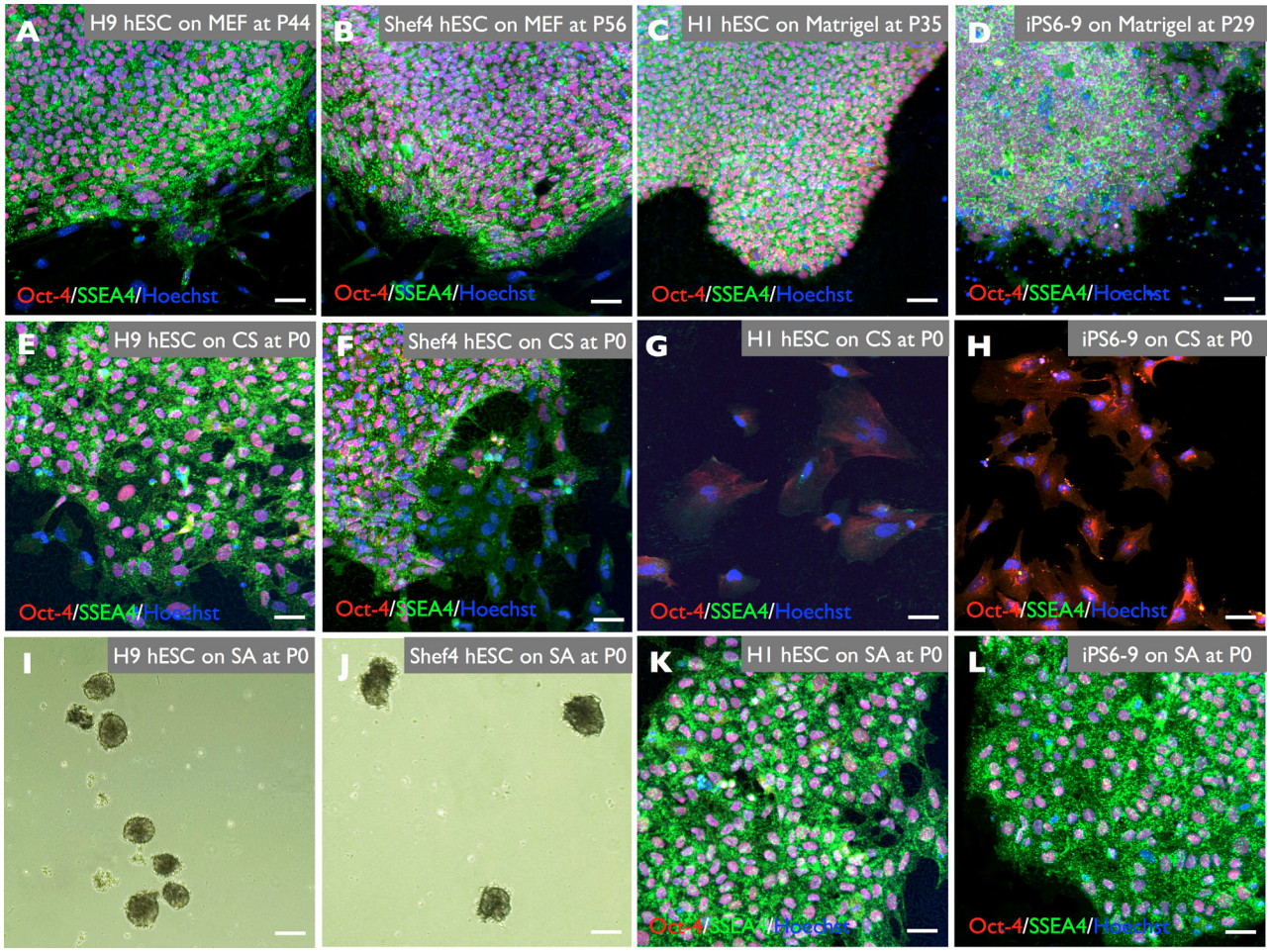

Figure 1. Transition preference of hESC/hiPSC onto xeno-free (XF) substrate CELLstart (CS) or StemAdhere (SA). (**A**) H9 hESC and (**B**) Shef4 hESC transitioned from MEF aggregated and detached from SA (**I,J**) but remained undifferentiated on CS (**E,F**), expressing the pluripotent nuclear marker Oct-4 and the cell surface marker SSEA4. (**C**) H1 hESC and (**D**) iPS6-9 cells transitioned from Matrigel remained undifferentiated on SA (**K,L**) but were differentiated on CS (**G,H**) substrate, expressing less Oct-4/SSEA4 and Oct-4 expression was no longer localized to the nucleus. All XF transitioned hESC/hiPSC were at P0 on CS (E–H) or SA (I–L). Scale bars = 50 μm.

approach, different cell lines exhibited different XF substrate preferences. As shown by retained normal colony morphology and Oct-4/SSEA4 expression, MEF-supported H9 hESC and Shef4 hESC (Fig. 1A,B) could only be stably transitioned to CELLstart matrix (Fig. 1E,F) but not StemAdhere, as clumps of cells were detached from the StemAdhere-coated surface (Fig. 1I,J). Conversely, Matrigel-supported H1 hESC and iPS6-9 (Fig. 1C,D) could only be stably transitioned to StemAdhere (Fig. 1K,L) but not CELLstart, as CELLstart colonies exhibited an increase in differentiated morphologies and decreased expression of Oct-4 and SSEA4 (Fig. 1G,H). This observation was incorporated into a schematic plan to transition hESC/hiPSC onto either CELLstart or StemAdhere XF substrate (Fig. 2).

We next tested the retention of pluripotency for transitioned cell lines cultured long-term in XF conditions. After more than seven passages under XF conditions, all lines retained robust expression of Oct-4 and SSEA4 (Fig. 3A–C) (H1 data not shown). Furthermore, real-time qPCR showed that H9 hESC (Fig. 3D), Shef4 hESC (Fig. 3E), and iPS6-9 (Fig. 3F) maintained under XF conditions up to P24, P27, and P7, respectively, retained Oct-4 and NANOG expression. Expression of Oct-4 and NANOG did not differ from H9 hESC, Shef4 hESC, or iPS6-9 cells that were maintained on MEF or Matrigel. Further analysis of germ lineage markers showed that XF transitioned hESC and hiPSC retained expression for ectodermal (NES, SOX2, PROM1, and PAX6), mesodermal (Brachyury and CD34), and endodermal (GATA4 and SOX17) markers, demonstrating that XF transitioned cells retained multigerm-layer potential (Fig. 3D–F). Also, XF conditions did not affect MKI67 expression, suggesting unaltered cell proliferation and expansion potential.

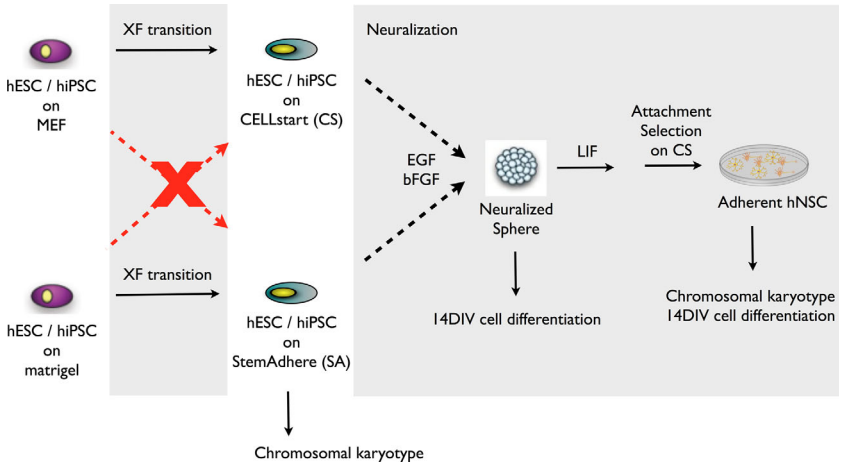

Figure 2. Xeno-free (XF) transition and neuralization of hESC and hiPSC to generate neuralized sphere and adherent hNSC.

Although XF culture conditions did not alter hESC/hiPSC pluripotency or proliferation, induction of karyotype abnormality under XF conditions is a potential concern for both transition and long-term cell passaging. As shown in Figure 3G–J, most lines (H9 hESC, Shef4 hESC, iPS6-9) retained normal karyotype after at least seven passages, demonstrating the feasibility for stable derivation of neural derivatives under the XF conditions described below. However, XF transitioned H1 hESC developed a trisomy of chromosome 20 (Fig. 3I); accordingly, this line was excluded from the remaining studies.

Neural derivatives generated from XF hESC and hiPSC retain normal karyotype

Having established XF substrate and media conditions for the transition and maintenance of hESC and hiPSC lines, we sought to generate neural derivatives from these cells, determine the gene expression profile of these derivatives for pluripotency, mesodermal, endodermal, and ectodermal markers, and assess karyotypic stability under XF conditions (Fig. 2). We termed these derivative populations neuralized spheres and adherent hNSC, respectively, as described below.

Neural induction of non-XF-transitioned, MEF-supported, hESC/hiPSC using defined neuralization media containing EGF/bFGF and B27/heparin has been previously reported (Ebert et al., 2009, 2013). In our studies, XF substrate and media transitioned H1, H9, and iPS6-9 neuralized spheres were generated using a similar but modified protocol in defined neural induction media containing B27/heparin. In parallel, XF transitioned Shef4 neuralized spheres were generated using XF neural induction media containing N2 supplement in lieu of B27/heparin, as proof of principal for neuralization feasibility under completely XF conditions. After three to six passages, all cell lines were either propagated as neuralized spheres, or transitioned to adherent monolayer conditions in XF hNSC media containing LIF, followed by attachment on CELLstart-coated substrate for propagation as adherent hNSC (Fig. 2).

Gene expression profile analysis of neuralized spheres and adherent hNSC revealed downregulation of the pluripotency markers Oct-4 and NANOG in comparison with undifferentiated hESC and hiPSC (Fig. 4A–C), consistent with lineage restriction. In parallel, mesodermal (Brachyury) and endodermal (GATA4 and SOX17) markers were generally downregulated in both neuralized spheres and adherent hNSC, consistent with neuralization of the starting pluripotent cell populations (Fig. 4A–C). However, CD34, a marker for the hematopoietic lineage as well as CNS resident microglial cells, was increased in neuralized spheres, and to a greater degree in adherent hNSC (Fig. 4A,C). PROM1, a marker for hematopoietic, neural, and other stem cells, was increased in neuralized spheres and adherent hNSC derived from H9 hESC and iPS6-9, but decreased in neuralized spheres and adherent hNSC derived from Shef4 hESC. Ectodermal lineage marker expression (NES, SOX2, and PAX6) was generally sustained in both neural derivative conditions, but exhibited line-to-line variability (Fig. 4A–C). Variations in these observations between lines could reflect overall differences in the balance of neural lineage commitment. Finally, both MKI67 and PCNA expression were maintained in both neuralized spheres and adherent hNSC, suggesting that expansion potential was maintained.

As described above for hESC/hiPSC, chromosomal instability is a concern when culture conditions are altered and cells are passaged over time. Karyotype

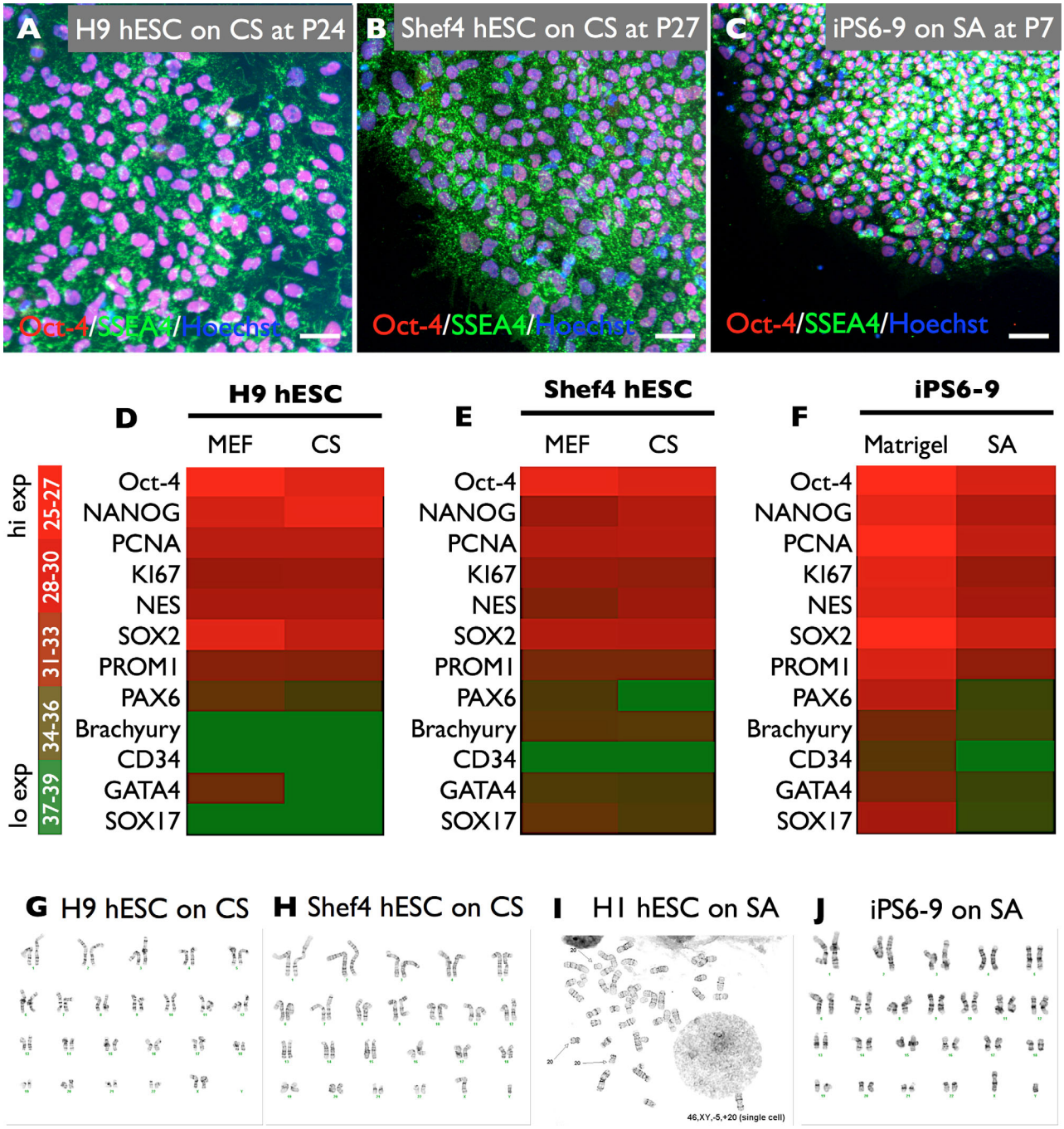

Figure 3. hESC and hiPSC retained pluripotency and normal karyotype after long-term passaging under XF conditions. **(A)** H9 hESC on CS, **(B)** Shef4 hESC on CS, and **(C)** iPS6-9 on SA retained undifferentiated stability and expressions of Oct-4 and SSEA4 after P24, P27, and P7, respectively, under XF conditions. Sustained pluripotency was confirmed by real-time PCR, showing minute changes in gene expression profile of **(D)** H9 hESC, **(E)** Shef4 hESC, and **(F)** iPS6-9 after long-term XF transition from MEF to CS, or Matrigel to SA. Furthermore, XF transition of hESC/hiPSC retained normal karyotype for H9 hESC **(G)** and Shef4 hESC **(H)** on CS and iPS6-9 on SA **(J)**. However, **(I)** H1 hESC on SA had one trisomy incidence of chromosome 20. Heat map of gene expression was represented by cycle threshold of real-time PCR reactions. Values were normalized to 18s mRNA levels. Scale bars = 50 μm in A–C.

assessment showed that neural induction of XF transitioned H9 hESC, Shef4 hESC, and iPS6-9 generated hNSC (at Passage M3) that retained normal karyotype under XF conditions (Fig. 4D–F). Furthermore, and as proof of principle, H9 hNSC were expanded long-term in XF culture conditions for over 6 months and were shown to have continued normal karyotype at Passage M27 (Fig. 10).

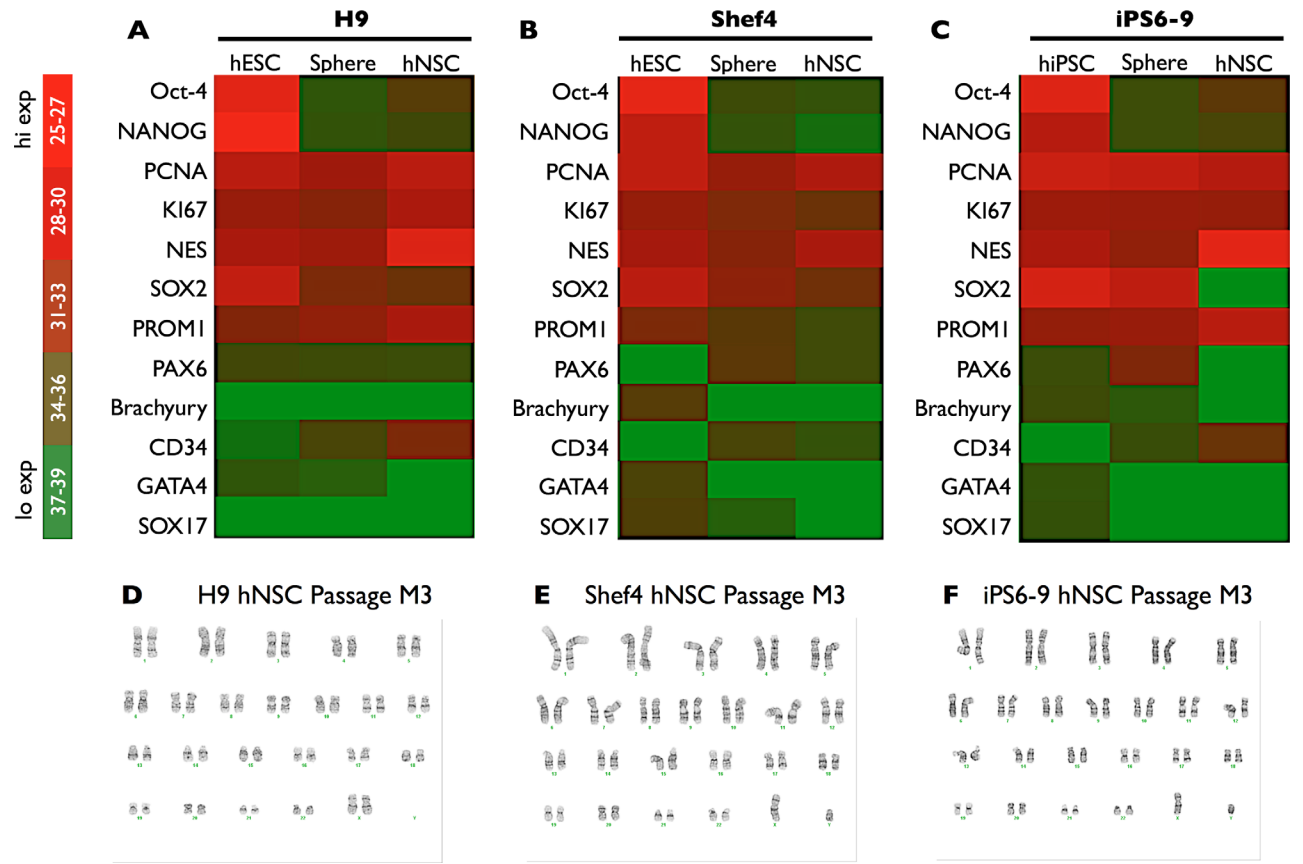

Figure 4. Gene expression of pluripotent markers Oct-4 and NANOG was reduced after **(A)** H9 hESC, **(B)** Shef4 hESC, and **(C)** iPS6-9 were differentiated into neuralized spheres or adherent hNSC under XF conditions. Furthermore, **(D)** H9, **(E)**, Shef4 and **(G)** iPS6-9 adherent hNSC retained normal karyotype after P3 under XF conditions. Heat map of gene expression was represented by cycle threshold of real-time PCR reactions. Values were normalized to 18s mRNA levels.

XF neural derivatives exhibit multipotent neural differentiation

The lack of robust upregulation of ectodermal markers in gene expression analyses following neuralization could reflect an early commitment stage of these neural derivative populations, making determination of the differentiation potential and profile of these cells an important variable. Accordingly, we dissociated neuralized spheres and passaged adherent hNSC, plated cells from these conditions at equal densities under identical differentiating conditions for 14DIV and assessed neural lineage marker expression, as described in the Materials and Methods.

Neuralized spheres generated from different pluripotent cell lines exhibited highly distinct patterns of β-tubulin III and GFAP expression under differentiating conditions. H9 and iPS6-9 neuralized sphere-dissociated cells exhibited scattered GFAP+ cells, with few β-tubulin III+ cells (Fig. 5A,C). Shef4 neuralized sphere-dissociated cells also exhibited scattered GFAP+ cells; however, in striking contrast, large numbers of β-tubulin III+ cells were readily detected (Fig. 5B). Furthermore, these lines exhibited dramatically variant cellular morphology, with a dense plexus of β-tubulin III positive fibers evident in Shef4 but not H9 or iPS6-9 neuralized sphere-dissociated cells. Neural lineage marker expressions as represented by cycle threshold heat map were generally consistent with immunocytochemical observations (Fig. 5D). H9 neuralized sphere-dissociated cells exhibited the lowest levels of neuronal marker expression. Shef4 neuralized sphere-dissociated cells exhibited higher overall expression levels of neuronal (BLBP, TUBB3, DCX, and SYN1) and astrocytic (GFAP and S100B) lineage genes in comparison with other lines based on cycle threshold (Fig. 5D; Table 2). This observation may suggest that Shef4 neuralized spheres exhibited a more differentiated and neuronally committed phenotype.

Adherent hNSC derived from H9, Shef4, and iPS6-9 also exhibited robust variations in the pattern of β-tubulin III and GFAP expression under differentiating conditions (Fig. 5E–G). Nearly all H9 adherent hNSC

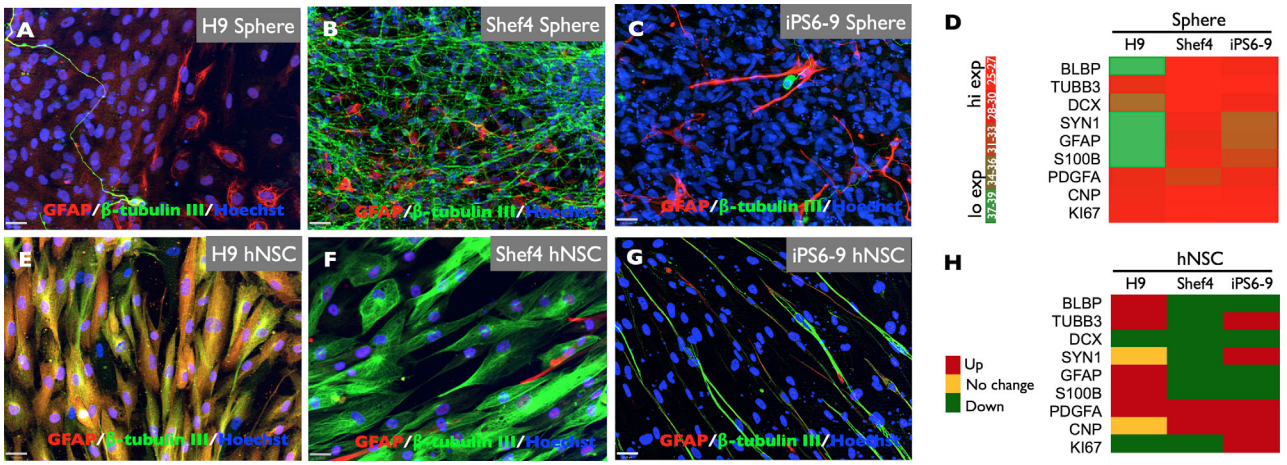

Figure 5. After 14DIV in differentiating conditions, **(A–C)** neuralized sphere-dissociated cells and **(E–G)** adherent hNSC derived from H9 hESC, Shef4 hESC, and iPS6-9 differentiated into cells expressing β-tubulin III (green) and GFAP (red). Real-time qPCR confirmed that after 14DIV differentiation, **(D)** H9, Shef4, and iPS6-9 neuralized sphere-dissociated cells had varying expression of markers associated with early radial glia (BLBP), neurons (TUBB3, DCX, SYN1), astrocytes (GFAP, S100B), oligodendrocytes (PDGFA, CNP), and cell proliferation (MKI67). Heat map of gene expression was represented by cycle threshold of real-time PCR reactions. Values were normalized to 18s mRNA levels. Changes to neural expression profile of **(H)** hNSC relative to neuralized sphere-dissociated cells after 14DIV differentiation are represented as upregulation (red), no change (yellow), and downregulation (green) for H9, Shef4, and iPS6-9 adherent hNSC. Scale bars = 50 μm in A–C,E–G

exhibited coexpression of both β-tubulin and GFAP (Fig. 5E). In contrast, Shef4 adherent hNSC exhibited a similar cellular morphology to the H9 line, with a flattened appearance and a large cytoplasm-to-nucleus ratio; further, β-tubulin III+ cells were rarely colocalized with GFAP (Fig. 5F,G). In striking contrast to both the H9 and Shef4 cell lines, iPS6-9 adherent hNSC exhibited relatively little evidence for either β-tubulin III or GFAP expression, with a majority of cells negative for both markers, absence of marker colocalization, and a distinct spindle-like morphology (Fig. 5F). Further assessment showed that all cell lines retained nestin expression after 14DIV under differentiating conditions (Fig. 6A–C), and that although many cells expressed the neuronal progenitor marker β-tubulin III described above (Fig. 5E–G), these cells lacked the expression of mature neuronal marker NeuN at this timepoint (Fig. 6D,E). In addition, immunocytochemistry also showed dramatic differences in morphology and neural marker expression between neuralized spheres and adherent hNSC (Fig. 5A–C,E–G). Real-time qPCR for neural lineage markers comparing adherent hNSC to neuralized spheres paralleled immunocytochemical observations (Fig. 5H). Of particular interest, oligodendroglial lineage genes (PDGFA and CNP) were generally upregulated in adherent hNSC for all cell lines (H9, Shef4, and iPS6-9)

TABLE 2.

Expression Profile of Neural Differentiation Associated Genes by Neuralized Sphere-Dissociated Cells and Adherent hNSC After 14DIV in Neural Differentiation Media

	Assay ID	Gene name	Gene description	Sphere			hNSC		
				H9	Shef4	iPS6-9	H9	Shef4	iPS6-9
Neuronal	Hs00361426_m1	BLBP	Brain lipid binding protein	ND	28.88	30.16	30.85	31.23	ND
	Hs00964962_g1	TUBB3	Neuronal Tubulin beta-3 chain	31.29	25.31	29.31	28.78	27.82	28.49
	Hs00167057_m1	DCX	Early neuronal doublecortin	ND	27.22	30.27	ND	32.71	32.12
	Hs00199577_m1	SYN1	Neuronal synapsin I	ND	30.34	34.38	ND	ND	32.87
Astrocytic	Hs00909236_m1	GFAP	Glial fibrillary acidic protein	ND	31.08	34.28	ND	34.66	ND
	Hs00902901_m1	S100B	S100 calcium binding protein B	ND	30.21	33.14	33.92	33.38	ND
Oligodendrocytic	Hs00234994_m1	PDGFA	Platelet-derived growth factor A	31.13	32.84	30.84	30.35	30.88	29.69
	Hs00263981_m1	CNP	2′,3′-Cyclic-nucleotide 3′-phosphodiesterase	30.70	29.63	29.95	30.68	29.24	28.48
Proliferation	Hs01032443_m1	MKI67	Nuclear protein Ki67	30.28	28.32	29.56	30.94	31.79	27.96

Expression values are shown by cycle threshold of real-time PCR reactions and normalized to 18s mRNA levels.

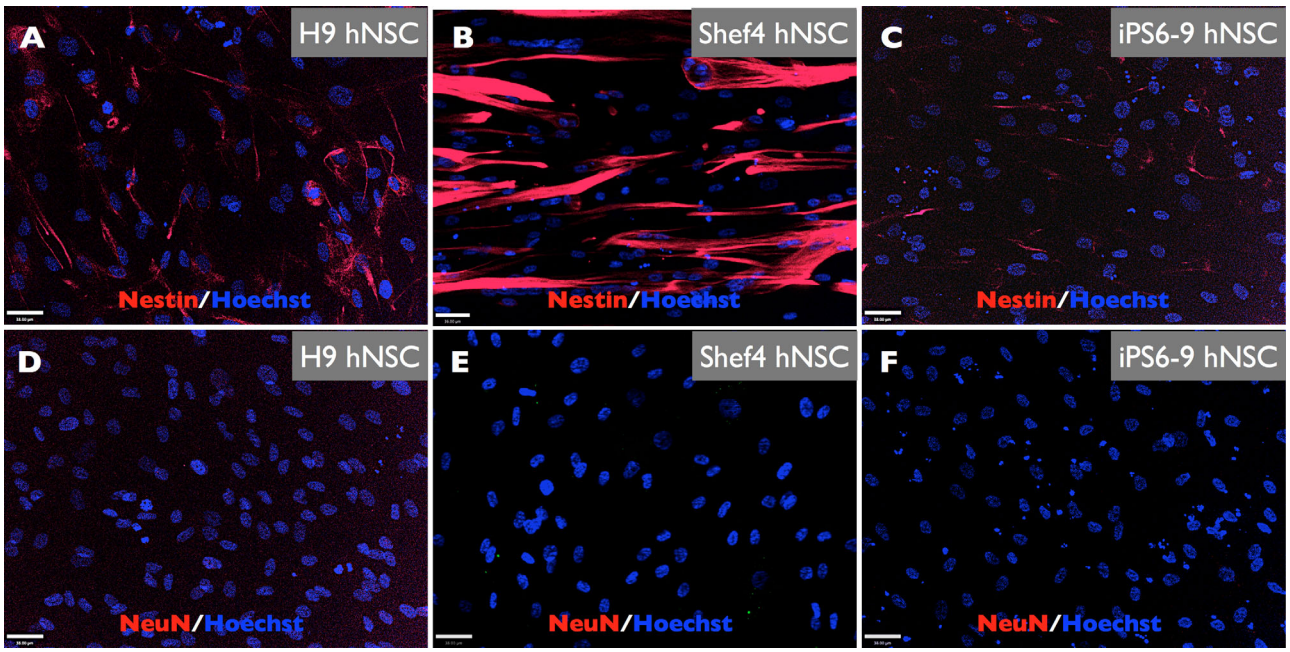

Figure 6. After 14DIV in differentiating conditions, only some of the cells in adherent H9 hNSC **(A)**, Shef4 hNSC **(B)**, and iPS6-9 hNSC **(C)** cultures expressed nestin, but not NeuN **(D–F)**. Scale bars = 38 μm.

in comparison to sphere-dissociated cells (Fig. 5H), suggesting a shifting of cell fate potential in adherent hNSC verses sphere-dissociated cells.

XF adherent hNSC exhibit enhanced oligodendroglial differentiation

We further evaluated the upregulation of oligodendroglial lineage genes in adherent hNSC versus sphere-dissociated cells using immunocytochemistry and quantitative flow cytometric analysis. While there are few cell surface makers for the neuronal and astroglial lineages, there are several well-characterized cell surface markers for the oligodendroglial lineage compatible with flow cytometry; accordingly, we selected O4 and GalC (Jackman et al., 2009; Nishiyama et al., 2009). As described in the Materials and Methods, we validated these markers by assessing the specificity of immunocytochemical staining. Immunocytochemistry of adherent hNSC (Fig. 7D–F) and neuralized sphere dissociated cells (Fig. 7A–C) maintained under differentiating conditions for 14DIV demonstrated that only adherent hNSC exhibited the potential to differentiate into O4+ oligoprogenitors (Fig. 7D–F). These O4+ oligoprogenitors lacked GalC expression (Fig. 7G–I), suggesting an early lineage commitment state (Fig. 7G–I). Because no O4 or GalC expression was detected in neuralized sphere dissociated cells after differentiation, we used quantitative flow cytometric analysis to compare the H9, Shef4, and iPS6-9 lines from adherent hNSC cultures for these markers, validating detection relative to isotype-matched IgG controls (Fig. 7J). Significant numbers of O4+ cells were detected in differentiated H9 (29.8% ± 4.9%), Shef4 (19.2% ± 1.7%) and iPS6-9 (24.3% ± 7.2%) adherent hNSC cultures (Fig. 7K). However, differentiation of adherent hNSC into mature GalC+ oligodendrocytes was relatively low (H9, 3.0% ± 0.2%; Shef4, 2.8% ± 0.7%; iPS6-9, 4.2% ± 0.3%) (Fig. 7L), showing that most oligoprogenitors were O4+/GalC−. No differences in the percentages of O4+ or GalC+ cells were detected among these three lines.

We next assessed whether adherent hNSC retained the capacity for proliferation after 14DIV under differentiating conditions, and in parallel, whether the identified oligoprogenitor population retained proliferative capacity, using EDU incorporation in combination with flow cytometry for the cell surface markers O4 and GalC. These data showed that 4.9% ± 0.2% of H9-derived adherent hNSC, 4.2% ± 0.5% of Shef4-derived adherent hNSC, and 2.0% ± 0.3% of iPS6-9 adherent hNSC exhibited continuing cell proliferation after 14DIV in differentiating conditions (Fig. 8A–D). Surprisingly, and with the exception of iPS6-9 adherent hNSC (Fig. 8G), proliferating H9 and Shef4 adherent hNSC were also O4+ (O4+/EDU+; Fig. 8E,F,H); including 4.1% ± 0.3% of H9 adherent hNSC and 3.9% ± 0.9% of Shef4

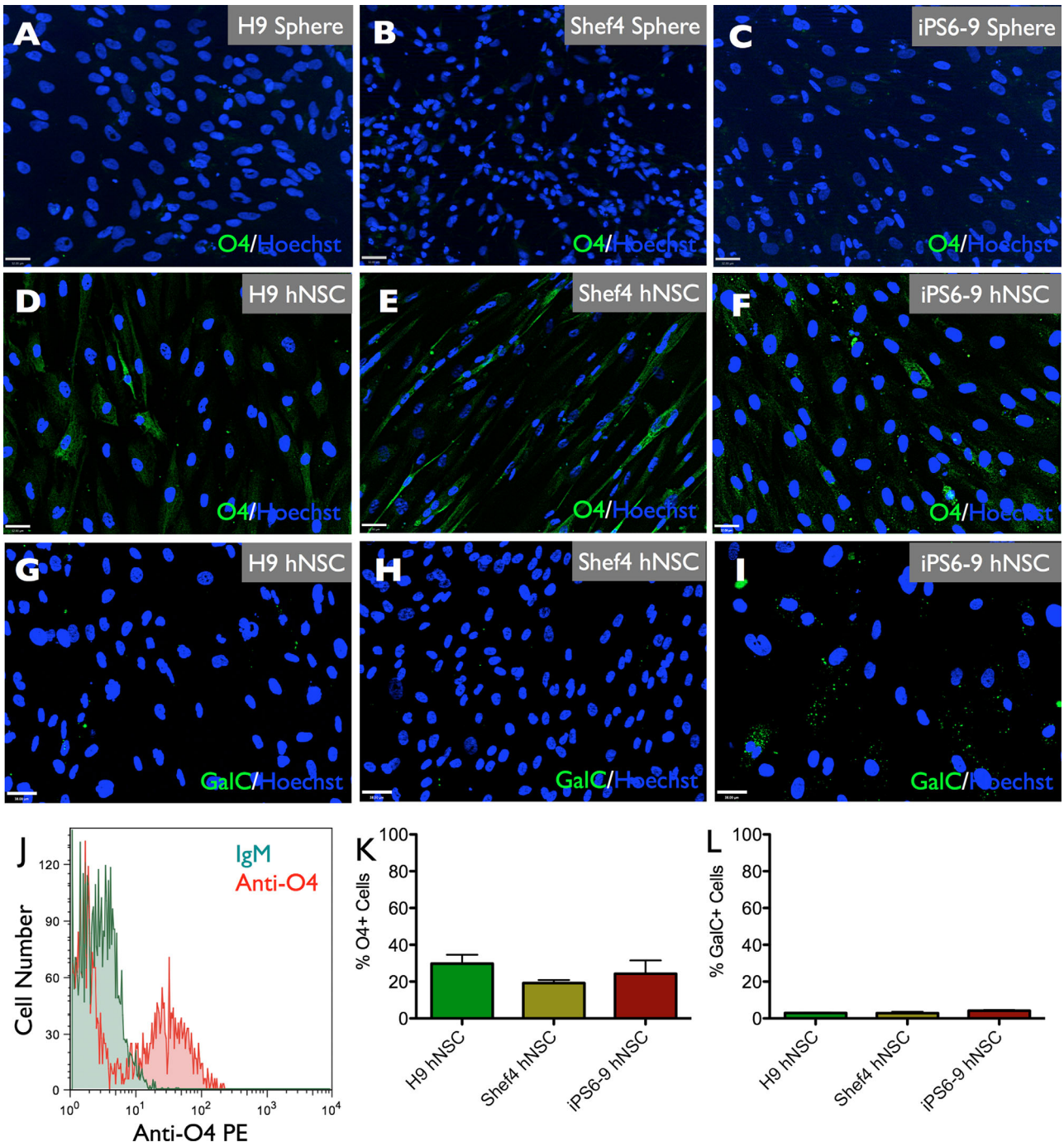

Figure 7. Under differentiating conditions, neuralized sphere-dissociated cells derived from **(A)** H9 hESC, **(B)** Shef4 hESC, and **(C)** iPS6-9 had no expression of the oligoprogenitor marker O4. Interestingly, **(D)** H9, **(E)** Shef4, and **(F)** iPS6-9 adherent hNSC had significant expression of O4, but not GalC **(G–I)** after 14DIV in differentiating conditions. Flow cytometric analysis using anti-O4 PE or anti-GalC A488 confirmed that adherent hNSC derived from H9, Shef4, and iPS6-9 expressed **(J,K)** O4 but **(L)** not GalC after 14DIV in differentiating conditions. Values of O4+ or GalC+ cells were expressed as percent (± SE) relative to (J) control IgG or IgM isotype labeled cells. No differences in (K) O4+ or (L) GalC+ cells between adherent hNSC lines were detected (one-way ANOVA with post-hoc Tukey's multiple comparison tests; $n = 3$; $P < 0.05$). Data reflect the average of three biological replicates (each with technical triplicates). Scale bars = 50 μm in A–I.

adherent hNSC. Accordingly, ~70–80% of EDU+ proliferating cells were O4+ oligoprogenitors for H9 and Shef4 adherent hNSC, compared to ~10% for iPS6-9 adherent hNSC (Fig. 9). Further, not all O4+ cells were proliferating, as 25.7%, 24.4%, and 24.1% of H9, Shef4, and iPS6-9, respectively, were O4+/EDU− (Fig. 8E–H).

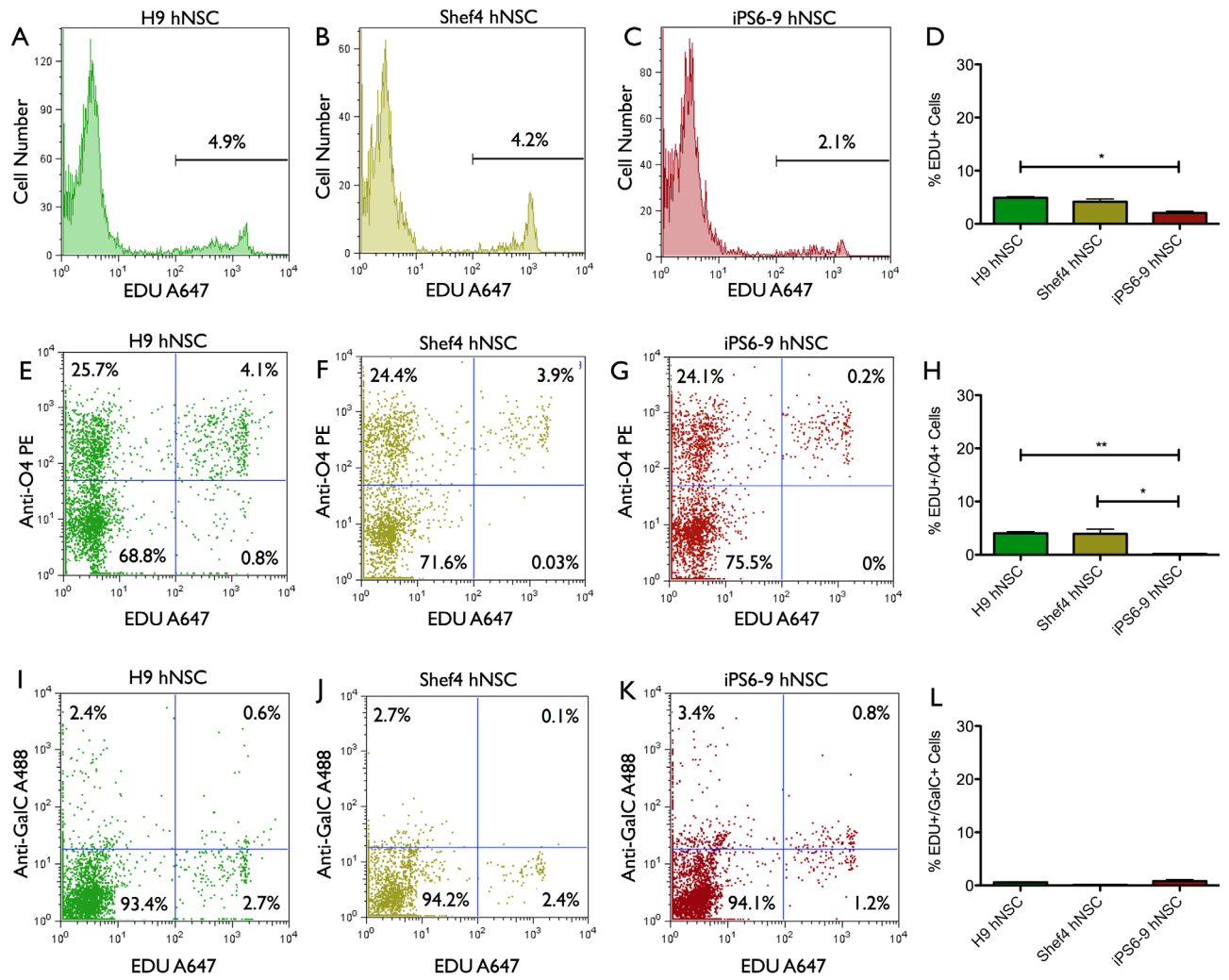

Figure 8. Under differentiating conditions, **(A)** H9, **(B)** Shef4, and **(C)** iPS6-9 adherent hNSC exhibited proliferation as illustrated by the representative histogram of **(D)** EDU incorporation. The majority of these proliferative EDU+ cells were also positive for **(H)** O4 but negative for **(L)** GalC after 14DIV in differentiating conditions, as shown by dot plots of H9 **(E,I)**, Shef4 **(F,J)** and iPS6-9 **(G,K)** adherent hNSC. All flow cytometric gates were set using control IgG or IgM isotype-labeled cells. Values of EDU+, O4+, or GalC+ cells are expressed as percent (± SE) relative to control IgG or IgM isotype-labeled cells. Data reflect the average of three biological replicates (each with technical triplicates). One-way ANOVAs with post-hoc Tukey's multiple comparison tests; $n = 3$; $^{*}P < 0.05$, $^{**}P < 0.01$.

These nonproliferating O4+ cells could represent quiescent OL progenitors or committed OL precursors that are no longer proliferating under differentiating conditions. This is consistent with the detected small number of GalC+/EDU− cells in H9 (2.4%), Shef4 (2.7%), and iPS6-9 (3.4%) adherent hNSC cultures (Fig. 8I–L), suggesting that most nonproliferating O4+ cells have not differentiated into mature oligodendrocytes under these conditions.

DISCUSSION

Methods of neuralization of pluripotent human stem cells are based largely on current knowledge of neural development during embryogenesis (Denham and Dottori, 2009). However, the neural derivatives generated in different protocols can exhibit variable fate potential, and may be at different stages along the developmental continuum. Furthermore, few studies have developed methods/protocols for efficient generation of neural derivatives or characterized neural multipotency, proliferation, and, critically, normal karyotype under completely XF conditions. In this study we demonstrated 1) a one-step XF transition protocol for hESC/hiPSC, 2) the neural derivation of neuralized spheres and adherent hNSC under XF conditions, and 3) the tripotent differentiation potential of these XF and chromosomal stable neural derivatives.

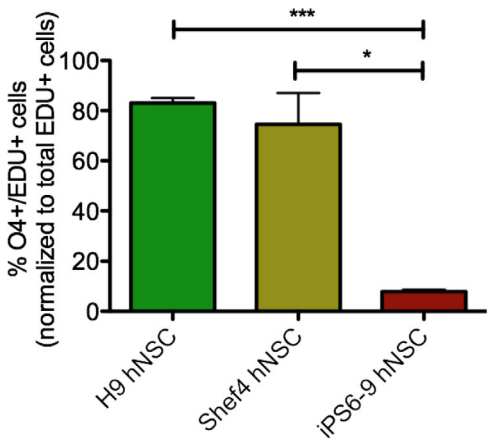

Figure 9. After 14DIV under differentiating conditions, the percent of proliferating oligoprogenitors (O4+/EDU+) normalized to total EDU+ proliferating cells for H9, Shef4, and iPS6-9 adherent hNSC was quantitatively assessed by flow cytometry. Data reflect the average of three biological replicates (each with technical triplicates). One-way ANOVA with post-hoc Tukey's multiple comparison tests; $n = 3$; $^{*}P < 0.05$, $^{***}P < 0.001$.

Neuralization via the formation of EBs/neural rosettes is a well-established method to generate tripotent neural derivatives; however, these derivatives have low expansion potential and are difficult to maintain under defined or XF conditions (Zhang et al., 2001; Pomp et al., 2005; Lee et al., 2007). Alternatively, we have adopted an EGF/bFGF neuralization method used previously to generate non-XF neural derivatives (Ebert et al., 2013) and modified this method to generate karyotypically normal neuralized spheres or adherent hNSC under XF conditions. XF substrate and media transition of hESC/hiPSC was tested using the XF hESC media/CELLstart matrix substrate and TeSR2 media/StemAdhere substrate systems. A novel observation from our results was the identification of a substrate preference by cell line. H9 hESC and Shef4 hESC, which were previously maintained on MEF, retained normal undifferentiated morphology, maintained pluripotency marker expression, and adherence only on CELLstart matrix. In contrast, H1 hESC and iPS6-9, which were previously maintained on Matrigel, retained normal undifferentiated morphology, maintained pluripotency marker expression, and adherence only on StemAdhere substrate. Substrate preference by cell line has not been reported previously, but is not entirely surprising, as CELLstart matrix was originally optimized by the manufacturer using MEF-supported hESC, while StemAdhere was optimized using Matrigel-supported hESC.

Using a combination of growth factors (EGF/bFGF/LIF) or attachment selection on CELLstart substrate, neuralized spheres and adherent hNSC were generated under defined or XF conditions. These neural derivatives were highly proliferative, retained normal karyotype, and expressed ectodermal markers (NES, SOX2, PROM1, and PAX6) consistent with neural lineage differentiation. Although both neuralized spheres and adherent hNSC had undetected expression levels of the mesodermal marker Brachyury and the endodermal markers GATA4 and SOX17, adherent hNSC exhibited increased hematopoietic CD34 expression compared to neuralized spheres and starting hESC/hiPSC pluripotent cell populations. During development, a CD34+ cell subpopulation occupies the CNS as resident microglia, which are capable of proliferating in response to infection, injury, and disease (Asheuer et al., 2004; Kettenmann et al., 2011). The observation of an increase in CD34 expression in neural derivatives was surprising, but could reflect either selection for 1) an undifferentiated cell population that retained some pre-neural potential to differentiate into microglia and recapitulate normal neural development, or 2) a neural transient CD34+ cell population that could give rise to cells of a neural lineage (Goolsby et al., 2003; Shyu et al., 2006; Zangiacomi et al., 2008).

Differentiation of neuralized sphere dissociated cells and adherent hNSC for 14DIV revealed variations in the pattern of neuronal β-tubulin III and astrocyte GFAP expression among cell lines, highlighting the intrinsic differences between these lines. Furthermore, few cells expressed mature/terminal differentiation markers (e.g., NeuN and GalC) after 14DIV differentiation, suggesting an early state of lineage commitment. Of particular interest, Shef4 neuralized spheres and adherent hNSC had the most robust neuronal β-tubulin III expression after 14DIV differentiation. Shef4 has previously been observed to exhibit a particularly high degree of neuronal differentiation (Dr. Harry Moore, pers. commun.), suggesting an intrinsic commitment to this cell type over the glial lineage, and consistent with the variation between lines observed here. However, our data suggest that this cell differentiation preference can be altered by the conditions under which neuralized derivatives of pluripotent cells are expanded; specifically, whether cultured as spheres versus adherent cells. It should also be noted that, in contrast to H9 and iPS6-9, Shef4 was exposed to a pure XF derivation paradigm in which XF N2 was substituted for B27 during initial sphere generation from pluripotent cells, as described above. Accordingly, the possibility that N2 components contributed to this observation cannot be excluded. Oligoprogenitor marker expression was observed only in differentiated adherent hNSC, but not in differentiated neuralized sphere-dissociated cells. This observation could reflect an effect of substrate

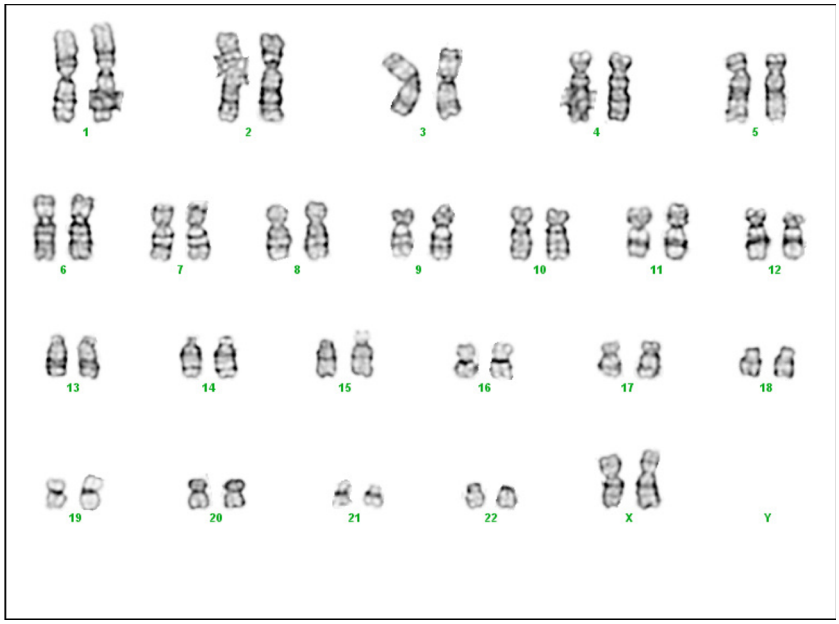

Figure 10. Extended passaging of adherent H9 hNSC (Passage M27) did not promote chromosomal instability.

properties in directly driving oligo lineage commitment, and/or a shift in the placement of cells under these conditions on the overall continuum of lineage commitment. As shown by cycle threshold in Table 2, adherent hNSC had an overall decrease in the expression of genes associated with neurons and astrocytes, and an overall increase in the expression of genes associated with oligodendrocytes relative to neuralized sphere-dissociated cells. Furthermore, and unlike neuronal β-tubulin III and astrocyte GFAP expression, we did not detect much variation in the percent of O4+ oligoprogenitors for H9, Shef4, and iPS6-9 adherent hNSC, as shown via immunocytochemistry and flow cytometric analysis. The lack of apparent variation in the pattern of oligodendroglial O4 expression in adherent hNSC (for all three lines) is interesting, and further suggests that neuralization under adherent conditions enhanced the potential to generate oligoprogenitors. However, further analysis of O4+ cell proliferation assessment via EDU incorporation showed significant differences between iPS6-9 adherent hNSC versus H9 and Shef4 adherent hNSC. Although such differences between hiPSC and hESC have been observed in a number of recent studies (Bilic and Izpisua Belmonte, 2012; Rada-Iglesias and Wysocka, 2011), they also suggest that intrinsic variations between cell lines are not overcome by a single neuralization protocol.

Selection for specific cell fates has been an important goal of many neuralization methods; however, chromosomal stability of neuralized derivatives has rarely been tested. Exposure of hESC to potent morphogens such as retinoic acid has been shown to increase the rate of aneuploidy by 2-fold (Sartore et al., 2011). Furthermore, long-term culture of human neural precursor cells for more than 9 weeks has been shown to increase susceptibility of chromosome 7 and 19 trisomy (Sareen et al., 2009), suggesting that the time in culture and the long-term passaging of neural derivatives may also increase the incidence of aneuploidy. We found that long-term XF maintenance and cell passaging resulted in stable, karyotypically normal cells lines in hESC/hiPSC cells up to P27 (see Fig. 3), and neural derivatives up to M27 (see Fig. 10). The single exception was XF transitioned H1 hESC; this may not be surprising, given that other investigators have found H1 hESC to be specifically sensitive to changes in culture conditions (Allegrucci and Young, 2007).

Overall, we have demonstrated the transition of multiple hESC and hiPSC lines onto XF substrate and media conditions, and established a reproducible neuralization protocol. These different cell fate potentials observed in several neural derivatives partly recapitulate normal neural development, and suggest the feasibility of neural differentiation under XF conditions. However, more work is needed to characterize and test the translational feasibility of these XF neural derivatives, particularly how they behave in an animal system, and how they respond to the cues and toxicity of the injury microenvironment in the CNS.

ACKNOWLEDGMENTS

We thank Dr. Harry Moore (University of Shefield, U.K.) for generously providing Shef4 hESC, and Priya Gohil, Sara Mohamed, Dennis Thai, Asaad Traina, Anna Tong, and Joel Trushinski for superb technical assistance.

CONFLICT OF INTEREST

None of the authors had any conflict of interest including any financial, personal, or other relationships with other people or organizations within 3 years of beginning the submitted work that could inappropriately influence, or be perceived to influence, their work.

ROLE OF AUTHORS

All authors had full access to all the data in the study and take responsibility for the integrity of the data and the accuracy of the data analysis. Study concept and design: HXN, DH, AJA, BJC. Acquisition of data: HXN, UN, GF, DM, DH, NK. Analysis and interpretation of data: HXN, GF, DM, UN, NK, BJC, AJA. Drafting of the article; HXN, AJA. Critical revision of the article for important intellectual content: HXN, AJA, BJC. Statistical analysis: HXN, UN. Obtained funding: HXN, AJA, BJC. Administrative, technical, and material support: HXN, AJA, DH, GF, DM, BJC. Study supervision: HXN, AJA.

LITERATURE CITED

Allegrucci C, Young LE. 2007. Differences between human embryonic stem cell lines. Hum Reprod Update13:103–120.

Asheuer M, Pflumio F, Benhamida S, Dubart-Kupperschmitt A, Fouquet F, Imai Y, Aubourg P, Cartier N. 2004. Human CD34+ cells differentiate into microglia and express recombinant therapeutic protein. Proc Natl Acad Sci U S A101:3557–3562.

Bergstrom R, Strom S, Holm F, Feki A, Hovatta O. 2011. Xeno-free culture of human pluripotent stem cells. Methods Mol Biol767:125–136.

Bilic J, Izpisua Belmonte JC. 2012. Concise review: induced pluripotent stem cells versus embryonic stem cells: close enough or yet too far apart? Stem Cells30:33–41.

Chambers SM, Fasano CA, Papapetrou EP, Tomishima M, Sadelain M, Studer L. 2009. Highly efficient neural conversion of human ES and iPS cells by dual inhibition of SMAD signaling. Nat Biotechnol27:275–280.

Chera B, Schaecher KE, Rocchini A, Imam SZ, Ray SK, Ali SF, Banik NL. 2002. Calpain upregulation and neuron death in spinal cord of MPTP-induced parkinsonism in mice. Ann N Y Acad Sci965:274–280.

Chiba S, Lee YM, Zhou W, Freed CR. 2008. Noggin enhances dopamine neuron production from human embryonic stem cells and improves behavioral outcome after transplantation into Parkinsonian rats. Stem Cells26:2810–2820.

Cobo F, Stacey GN, Hunt C, Cabrera C, Nieto A, Montes R, Cortes JL, Catalina P, Barnie A, Concha A. 2005. Microbiological control in stem cell banks: approaches to standardisation. Appl Microbiol Biotechnol68:456–466.

Denham M, Dottori M. 2009. Signals involved in neural differentiation of human embryonic stem cells. Neurosignals17:234–241.

Ebert AD, Yu J, Rose FF Jr, Mattis VB, Lorson CL, Thomson JA, Svendsen CN. 2009. Induced pluripotent stem cells from a spinal muscular atrophy patient. Nature457:277–280.

Ebert AD, Shelley BC, Hurley AM, Onorati M, Castiglioni V, Patitucci TN, Svendsen SP, Mattis VB, McGivern JV, Schwab AJ, et al. 2013. EZ spheres: a stable and expandable culture system for the generation of pre-rosette multipotent stem cells from human ESCs and iPSCs. Stem Cell Res10:417–427.

Erceg S, Lainez S, Ronaghi M, Stojkovic P, Perez-Arago MA, Moreno-Manzano V, Moreno-Palanques R, Planells-Cases R, Stojkovic M. 2008. Differentiation of human embryonic stem cells to regional specific neural precursors in chemically defined medium conditions. PLoS One3:e2122.

Erceg S, Ronaghi M, Oria M, Rosello MG, Arago MA, Lopez MG, Radojevic I, Moreno-Manzano V, Rodriguez-Jimenez FJ, Bhattacharya SS, et al. 2013. Transplanted oligodendrocytes and motoneuron progenitors generated from human embryonic stem cells promote locomotor recovery after spinal cord transection. Stem Cells28:1541–1549.

Findikli N, Kahraman S, Akcin O, Sertyel S, Candan Z. 2005. Establishment and characterization of new human embryonic stem cell lines. Reprod Biomed Online10:617–627.

Goolsby J, Marty MC, Heletz D, Chiappelli J, Tashko G, Yarnell D, Fishman PS, Dhib-Jalbut S, Bever CT Jr, Pessac B, Trisler D. 2003. Hematopoietic progenitors express neural genes. Proc Natl Acad Sci U S A100:14926–14931.

Guillaume DJ, Zhang SC. 2008. Human embryonic stem cells: a potential source of transplantable neural progenitor cells. Neurosurg Focus24:E3.

Hatch MN, Nistor G, Keirstead HS. 2009. Derivation of high-purity oligodendroglial progenitors. Methods Mol Biol549:59–75.

Jackman N, Ishii A, Bansal R. 2009. Oligodendrocyte development and myelin biogenesis: parsing out the roles of glycosphingolipids. Physiology (Bethesda)24:290–297.

Jouhilahti EM, Peltonen S, Peltonen J. 2008. Class III beta-tubulin is a component of the mitotic spindle in multiple cell types. J Histochem Cytochem56:1113–1119.

Kettenmann H, Hanisch UK, Noda M, Verkhratsky A. 2011. Physiology of microglia. Physiol Rev91:461–553.

Kohen NT, Little LE, Healy KE. 2009. Characterization of Matrigel interfaces during defined human embryonic stem cell culture. Biointerphases4:69–79.

Lee G, Kim H, Elkabetz Y, Al Shamy G, Panagiotakos G, Barberi T, Tabar V, Studer L. 2007. Isolation and directed differentiation of neural crest stem cells derived from human embryonic stem cells. Nat Biotechnol25:1468–1475.

Leroy K, Duyckaerts C, Bovekamp L, Muller O, Anderton BH, Brion JP. 2001. Increase of adenomatous polyposis coli immunoreactivity is a marker of reactive astrocytes in Alzheimer's disease and in other pathological conditions. Acta Neuropathol102:1–10.

Li XJ, Du ZW, Zarnowska ED, Pankratz M, Hansen LO, Pearce RA, Zhang SC. 2005. Specification of motoneurons from human embryonic stem cells. Nat Biotechnol23:215–221.

Martin MJ, Muotri A, Gage F, Varki A. 2005. Human embryonic stem cells express an immunogenic nonhuman sialic acid. Nat Med11:228–232.

McClain CR, Sim FJ, Goldman SA. 2012. Pleiotrophin suppression of receptor protein tyrosine phosphatase-beta/zeta maintains the self-renewal competence of fetal human oligodendrocyte progenitor cells. J Neurosci32:15066–15075.

Nagaoka M, Si-Tayeb K, Akaike T, Duncan SA. 2010. Culture of human pluripotent stem cells using completely defined conditions on a recombinant E-cadherin substratum. BMC Dev Biol10:60.

Nguyen HX, Tidball JG. 2003. Interactions between neutrophils and macrophages promote macrophage killing of rat muscle cells in vitro. J Physiol547:125–132.

Nishiyama A, Komitova M, Suzuki R, Zhu X. 2009. Polydendrocytes (NG2 cells): multifunctional cells with lineage plasticity. Nat Rev Neurosci10:9–22.

Okamura RM, Lebkowski J, Au M, Priest CA, Denham J, Majumdar AS. 2007. Immunological properties of human embryonic stem cell-derived oligodendrocyte progenitor cells. J Neuroimmunol192:134–144.

Okuno T, Nakayama T, Konishi N, Michibata H, Wakimoto K, Suzuki Y, Nito S, Inaba T, Nakano I, Muramatsu S, et al. 2009. Self-contained induction of neurons from human embryonic stem cells. PLoS One4:e6318.

Pomp O, Brokhman I, Ben-Dor I, Reubinoff B, Goldstein RS. 2005. Generation of peripheral sensory and sympathetic neurons and neural crest cells from human embryonic stem cells. Stem Cells23:923–930.

Rada-Iglesias A, Wysocka J. 2011. Epigenomics of human embryonic stem cells and induced pluripotent stem cells: insights into pluripotency and implications for disease. Genome Med3:36.

Rajala K, Lindroos B, Hussein SM, Lappalainen RS, Pekkanen-Mattila M, Inzunza J, Rozell B, Miettinen S, Narkilahti S, Kerkela E, et al. 2010. A defined and xeno-free culture method enabling the establishment of clinical-grade human embryonic, induced pluripotent and adipose stem cells. PLoS One5:e10246.

Sareen D, McMillan E, Ebert AD, Shelley BC, Johnson JA, Meisner LF, Svendsen CN. 2009. Chromosome 7 and 19 trisomy in cultured human neural progenitor cells. PLoS One4:e7630.

Sartore RC, Campos PB, Trujillo CA, Ramalho BL, Negraes PD, Paulsen BS, Meletti T, Costa ES, Chicaybam L, Bonamino MH, et al. 2011. Retinoic acid-treated pluripotent stem cells undergoing neurogenesis present increased aneuploidy and micronuclei formation. PLoS One6:e20667.

Schwartz CM, Tavakoli T, Jamias C, Park SS, Maudsley S, Martin B, Phillips TM, Yao PJ, Itoh K, Ma W, et al. Stromal factors SDF1alpha, sFRP1, and VEGFD induce dopaminergic neuron differentiation of human pluripotent stem cells. J Neurosci Res90:1367–1381.

Shyu WC, Lin SZ, Chiang MF, Su CY, Li H. 2006. Intracerebral peripheral blood stem cell (CD34+) implantation induces neuroplasticity by enhancing beta1 integrin-mediated angiogenesis in chronic stroke rats. J Neurosci26:3444–3453.

Skottman H, Hovatta O. 2006. Culture conditions for human embryonic stem cells. Reproduction132:691–698.

Sundberg M, Hyysalo A, Skottman H, Shin S, Vemuri M, Suuronen R, Narkilahti S. 2011. A xeno-free culturing protocol for pluripotent stem cell-derived oligodendrocyte precursor cell production. Regen Med6:449–460.

Swistowski A, Zeng X. 2012. Scalable Production of Transplantable Dopaminergic Neurons from hESCs and iPSCs in Xeno-Free Defined Conditions. Curr Protoc Stem Cell Biol Chapter 2, Unit2D 12.

Swistowski A, Peng J, Han Y, Swistowska AM, Rao MS, Zeng X. 2009. Xeno-free defined conditions for culture of human embryonic stem cells, neural stem cells and dopaminergic neurons derived from them. PLoS One4: e6233.

Wada T, Honda M, Minami I, Tooi N, Amagai Y, Nakatsuji N, Aiba K. 2009. Highly efficient differentiation and enrichment of spinal motor neurons derived from human and monkey embryonic stem cells. PLoS One4:e6722.

Xue Y, Cai X, Wang L, Liao B, Zhang H, Shan Y, Chen Q, Zhou T, Li X, Hou J, et al. 2013. Generating a non-integrating human induced pluripotent stem cell bank from urine-derived cells. PLoS One8:e70573.

Zangiacomi V, Balon N, Maddens S, Lapierre V, Tiberghien P, Schlichter R, Versaux-Botteri C, Deschaseaux F. 2008. Cord blood-derived neurons are originated from CD133+/CD34 stem/progenitor cells in a cell-to-cell contact dependent manner. Stem Cells Dev17:1005–1016.

Zhang XQ, Zhang SC. 2010. Differentiation of neural precursors and dopaminergic neurons from human embryonic stem cells. Methods Mol Biol584:355–366.

Zhang SC, Wernig M, Duncan ID, Brustle O, Thomson JA. 2001. In vitro differentiation of transplantable neural precursors from human embryonic stem cells. Nat Biotechnol19:1129–1133.